2018

Inhibitory Effects of Toll-Like Receptor 4, NLRP3 Inflammasome, and Interleukin-1β on White Adipocyte Browning

Meshail Okla
King Saud University, meokla@ksu.edu.sa

Walid Zaher
King Saud University

Musaad Alfayez
King Saud University

Soonkyu Chung
University of Nebraska-Lincoln, schung4@unl.edu

HHS Public Access

Author manuscript

Inflammation. Author manuscript; available in PMC 2018 July 30.

Published in final edited form as:

Inflammation. 2018 March ; 41(2): 626–642. doi:10.1007/s10753-017-0718-y.

Inhibitory Effects of Toll-Like Receptor 4, NLRP3 Inflammasome, and Interleukin-1β on White Adipocyte Browning

Meshail Okla[iD,1,2,6], **Walid Zaher**[3,4], **Musaad Alfayez**[5], and **Soonkyu Chung**[1]

[1]Department of Nutrition and Health Sciences, University of Nebraska-Lincoln, Lincoln, NE, USA

[2]Department of Community Health Sciences, College of Applied Medical Sciences, King Saud University, 183T11, P.O. Box 22452, Riyadh, 11495, Saudi Arabia

[3]College of Medicine Research Center, College of Medicine, King Saud University, Riyadh, Saudi Arabia

[4]Department of Anatomy, College of Medicine, King Saud University, Riyadh, Saudi Arabia

[5]Stem Cell Unit, Department of Anatomy, College of Medicine, King Saud University, Riyadh, Saudi Arabia

Abstract

Adipose tissue expansion is accompanied by infiltration and accumulation of pro-inflammatory macrophages, which links obesity to pathologic conditions such as type 2 diabetes. However, little is known regarding the role of pro-inflammatory adipose tissue remodeling in the thermogenic activation of brown/beige fat. Here, we investigated the effect of pattern recognition receptors (PRR) activation in macrophages, especially the toll-like receptor 4 (TLR4) and Nod-like receptor 3 (NLRP3), on white adipocyte browning. We report that TLR4 activation by lipopolysaccharide repressed white adipocyte browning in response to β3-adrenergic receptor activation and caused ROS production and mitochondrial dysfunction, while genetic deletion of TLR4 protected mitochondrial function and thermogenesis. In addition, activation of NLRP3 inflammasome in macrophages attenuated UCP1 induction and mitochondrial respiration in cultures of primary adipocytes, while the absence of NLRP3 protected UCP1 in adipocytes. The effect of NLRP3 inflammasome activation on browning was mediated by IL-1β signaling, as blocking IL-1 receptor in adipocytes protected thermogenesis. We also report that IL-1β interferes with thermogenesis *via*

[6]To whom correspondence should be addressed at Department of Community Health Sciences, College of Applied Medical Sciences, King Saud University, 183T11, P.O. Box 22452, Riyadh, 11495, Saudi Arabia. meokla@ksu.edu.sa.
Meshail Okla http://orcid.org/0000-0003-4855-243X

Electronic supplementary material The online version of this article (https://doi.org/10.1007/s10753-017-0718-y) contains supplementary material, which is available to authorized users.

Author Contributions M.O. designed and performed experiments, analyzed data, and wrote the manuscript. W.Z. and M.A. critically reviewed the manuscript. S.C. provided scientific guidance, participated in discussions and manuscript preparation, and helped in interpreting the significance of the results.

COMPLIANCE WITH ETHICAL STANDARDS

All protocols and procedures were approved by the Institutional Animal Care and Use Committee (IACUC) at the University of Nebraska-Lincoln in Nebraska, United States, and by the Institutional Review Board (IRB) at King Saud University in Riyadh, Saudi Arabia.

Conflicts of Interest.

The authors declare that they have no conflicts of interest.

oxidative stress stimulation and mitochondrial dysfunction as we observed a statistically significant increase in ROS production, decrease in SOD enzyme activity, and increase in mitochondrial depolarization in adipocytes treated with IL-1β. Collectively, we demonstrated that inflammatory response to obesity, such as TLR4 and NLRP3 inflammasome activation as well as IL-1β secretion, attenuates β3-adrenoreceptor-induced beige adipocyte formation *via* oxidative stress and mitochondrial dysfunction. Our findings provide insights into targeting innate inflammatory system for enhancement of the adaptive thermogenesis against obesity.

Keywords

TLR4; NLRP3 inflammasome; IL-1β; uncoupling protein 1; beige adipocytes; brown adipocytes; β3-adrenergic receptor

INTRODUCTION

Innate immunity comprises the non-specific arm of the immune system and it is closely intertwined with the adipose tissue remodeling [1]. The role of innate immune cells, such as anti-inflammatory M2 macrophages, eosinophils, and type 2 innate lymphoid cells, in the process of white adipose tissue (WAT) browning was previously studied [1–6]. Cold exposure promotes alternative activation of adipose tissue macrophages, which produce catecholamine for local browning stimulation, by mechanisms linked to cold-induced eosinophils recruitment and type 2 cytokines, interleukin (IL)-4 and IL-13 signaling [1–6]. Previous studies on eosinophil depletion demonstrated impaired beigeing of the subcutaneous white adipose tissue (sWAT) in response to a cold challenge [3, 6]. The type 2 innate lymphoid cells play a key role in eosinophil maintenance in adipose tissue and thus are crucial in thermogenesis [6]. Stimulation of type 2 innate lymphoid cells by IL-33 results in IL-5 production, which in turn stimulates eosinophil secretion of IL-4 to induce commitment to the beige adipocyte lineage [6]. Several immune cell subpopulations have been identified in the adipose tissue browning [1–6]; however, more research is needed to determine how the sympathetic nervous system and immune system interact and to understand the contribution of other immune cells, such as basophils, neutrophils, natural killers, and mast cells, in the browning process. Although several studies have pointed to the role of type 2 immune cells in the browning of WAT, little is known about the role of pro-inflammatory cells, such as M1 macrophages and pro-inflammatory cytokines in adaptive thermogenesis [1].

Brown and white adipose tissues play distinct roles in maintaining whole-body energy homeostasis. Brown fat dissipates large amounts of chemical energy as heat, and its activation exerts anti-obesity and anti-diabetic effects [2]. Numerous reports demonstrated an inverse relationship between brown fat activity and adiposity even in adult human [1, 7–11]. In addition, genetic- [12] and diet-induced models of obese mice [1, 13] showed suppressed thermogenic markers in the brown/beige fat. Given that inflammation is a hallmark of obesity [1, 14], obesity may prevent “browning” of the white fat due to pro-inflammatory type 1 immune system activation. In white adipocytes, pro-inflammatory cytokines derived from lipopolysaccharide (LPS)- or tumor necrosis factor α (TNF-α)-

activated macrophages suppressed the induction of the uncoupling protein 1 (UCP1) promoter activity and mRNA expression *via* extracellular signal-related kinase (ERK) activation [15]. Furthermore, IL-1β, a typical pro-inflammatory cytokine, suppressed isoproterenol-induced activation of the UCP1 promoter and cold-induced UCP1 expression in mouse adipose tissue [16]. These studies indicate that inflammation links obesity and dysfunctional thermogenesis; however, the nature of the link between obesity-associated chronic immune response and non-shivering thermogenesis is not fully understood.

Understanding the metabolic effect of inflammatory signaling on brown/beige adipocytes is crucial as there is a renewed interest in utilizing brown fat therapeutic potential for treating obesity and its associated metabolic diseases. The present study attempted to address whether differential inflammatory cues could affect β3-adrenergic receptor (β3-AR)-induced WAT browning. We tested whether activation of pattern recognition receptors (PRR), Toll-like receptors (TLR), and nucleotide-oligomerization domain-containing proteins (NOD)-like receptors (NLR) decreases adaptive thermogenesis and mitochondrial function by using TLR4 and NLRP3 loss-of-function mutant mice and primary human adipocytes. Using these approaches, we revealed that inflammation induces oxidative stress and mitochondrial dysfunction in adipocytes and, thus, represses β3-AR-induced white adipocyte browning.

MATERIALS AND METHODS

Chemicals

Fetal bovine serum (FBS) was purchased from GIBCO. Rosiglitazone (BRL 49653) was purchased from Cayman Chemical. Lipopolysaccharides (LPS) from *Escherichia coli* 055:B5 (3×10^6 endotoxin unit (EU)/mg), dibutyryl (Bt_2)-cAMP, insulin, and 3-isobutyl-1-methylxanthine (IBMX) were purchased from Sigma-Aldrich. Recombinant human and mouse IL-1β proteins were purchased from R&D Systems. IL-1 receptor antagonist (IL-1RA 407616) was purchased from Merck Millipore. β3-adrenergic receptor agonist (CL 316,243) was purchased from Santa Cruz.

Animals

All protocols and procedures were approved by the Institutional Animal Care and Use Committee (IACUC) at the University of Nebraska-Lincoln in Nebraska, United States, and King Saud University in Riyadh, Saudi Arabia. C57BL/6 male mice were purchased at 6 weeks of age from Jackson Laboratory. For LPS-mediated TLR4 activation, C57BL/6 male mice at 6–8 weeks of age (n = 6–8 per group) were injected intraperitoneally with *Escherichia coli* LPS (7.5 μg/mouse, equivalent to 22,500 EU) in saline (0.9% NaCl) every other day for 2 weeks. Saline was used as a vehicle for the control group. To stimulate thermogenesis, mice received intraperitoneal (i.p.) injections of CL 316,243 (CL) (1 mg/kg body weight) for the last 10 days before necropsy. The homozygous knockout for TLR4 expression (TLR4$^{-/-}$, B6. B10ScN-*Tlr4lps-del*/JthJ) and NLRP3 (Nlrp3$^{-/-}$, B6.129S6-*Nlrp3tm1Bhk*/J) were purchased from Jackson Laboratory and bred at ambient temperature. All experiments were conducted on male mice at 6–8 weeks of age (n = 6–8 per group). At the time of necropsy, inguinal fat was collected, snap frozen in liquid nitrogen, and kept at − 80 °C until analysis.

Body Surface Temperature

For the detection of thermal release, an infrared (IR) camera (A655sc, FLIR Systems) was used to acquire images of body surface temperature as we described previously [13]. Mean surface temperature in Fig. 1b was calculated by following the method of Crane et al. [17].

Hematoxylin and Eosin Staining

Inguinal adipose tissue samples from C57BL/6 and TLR4 KO mice were fixed immediately in 10% buffered formalin. Paraffin-embedded adipose tissue samples were sectioned into 10 μm thickness for hematoxylin and eosin (H&E) staining.

RNA Isolation, cDNA Synthesis, and Real-time qPCR

Total RNA was extracted using Trizol reagent (Invitrogen) according to the manufacturer's instructions and RNA was isolated using chloroform-isopropanol method. To remove genomic DNA contamination, RNA was purified using DNase (5 PRIME). Two micrograms of RNA was reverse-transcribed into cDNA in a total volume of 20 μL using iScript cDNA synthesis kit (Bio-Rad). Gene expression analysis was determined by qPCR (QuantStudio 6, Applied Biosystems), and relative gene expression was normalized to 36B4. Gene-specific primers for qPCR were obtained from Integrated DNA Technologies (Chicago, IL, USA) and the complete gene lists can be found in Supplementary Table 1.

Preparation and Treatment of Cultures of Primary Adipocytes

For cultures of primary human adipocytes, abdominal subcutaneous adipose tissues were obtained from females with a body mass index of ~ 30 kg/m^2 during liposuction or abdominoplasty surgery. All protocols and procedures were approved by the Institutional Review Board at the University of Nebraska-Lincoln and King Saud University. Isolation of human adipose-derived stem cells (*h*ASC) and differentiation of adipocytes were conducted as we described previously [18]. For cultures of primary mouse adipocytes, subcutaneous fat-derived stem cells were used and differentiated as we described previously [13]. In some experiments, ear mesenchymal stem cells (EMSC) were used as described previously [13]. For LPS treatment, adipocytes were incubated with LPS (100 ng/ml) for 48–72 h followed by Bt_2-cAMP (0.5–0.7 mM) for 6–12 h or NE (1 μM) for 12 h.

BMP7 Preparation and Treatment

We infected *h*ASC with BMP7 adenovirus (a generous gift from Tong Chuan He at the University of Chicago Medical Center) and we collected conditioned medium as we described previously [18]. Before inducing adipogenic differentiation, *h*ASC were grown with or without BMP7-conditioned medium containing ~ 100 ng/ml of BMP7. After 3 days of BMP7 incubation (~ 100 ng/ml), *h*ASC were subjected to adipogenic differentiation cocktail as described before [18]. During adipocyte culturing, ~ 100 ng/ml of BMP7 was maintained by adding fresh conditioned medium every 3 days.

Transmission Electron Microscopy

Perfusion fixation was applied on C57BL/6 mice injected with either saline, CL, or LPS +CL. Small tissue fragments of inguinal fat were fixed in 2% glutaraldehyde and 2%

paraformaldehyde in 0.1 M phosphate buffer. Fixed samples were embedded in epoxy resin and sectioned for electron microscopy observation.

Mitochondrial PCR Array

The Mouse Mitochondrial RT^2 Profiler™ PCR Array (QIAGEN) was used according to the manufacturer's protocol by real-time PCR. Pools of equal amounts of total RNA were obtained from inguinal fat of CL or LPS+CL-injected mice ($n = 6$). The results were analyzed using software provided by QIAGEN.

mtDNA Quantification by qPCR

Genomic DNA was isolated using DNAzol (Life Technologies) from homogenized subcutaneous fat tissues from either wild-type or TLR4 KO mice. Quantitative PCR was performed for mtDNA analysis as we described previously [13].

Oxygen Consumption Rate by Seahorse

To determine mitochondrial respiration, oxygen consumption rate (OCR) was measured using an XF24 Extracellular Flux analyzer (Seahorse) as we described previously [19]. Measurements were performed at the basal level and after injection of three compounds affecting bioenergetics: 1 μM Oligomycin (oligo) (Sigma), 2 μM carbonyl cyanide 4-trifluoromethoxy phenylhydrazone (FCCP) (Sigma), and 0.5 μM Antimycin A plus Rotenone (AA+Rot) (Sigma). Upon completion of the Seahorse XF24 Flux analysis, cells were lysed to measure the protein concentration using BCA assay (Pierce). The results were normalized with the protein content of corresponding well and the data were presented as a function of time or as a percentage of baseline respiration.

Mitochondrial Membrane Potential Measurement by Flow Cytometry

Changes in mitochondrial membrane potential ($\Delta\psi m$) were measured by using Muse MitoPotential Assay kit (Merck Millipore) and Muse Flow Cytometry (Merck Millipore) following the manufacturer's protocol. A MitoPotential Dye, a cationic and lipophilic dye, was used to detect changes in the mitochondrial membrane potential and 7-AAD was used as an indicator of cell death. The percentage of total depolarized cells is a sum of depolarized live and depolarized dead cells.

Cellular Reactive Oxygen Species Detection

A commercial kit of DCFDA (2,7-dichloro-dihydrofluorescein diacetate) (Cayman) was used to measure the intracellular reactive oxygen species (ROS) level as we described previously [13]. Oxidation of DCFDA to the highly fluorescent 2,7-dichloro-fluorescein (DCF) is proportionate to ROS generation. Fluorescence intensity was measured by Synergy H1 (Bio-Rad) at Ex 485 nm and Em 528 nm kinetically every 50 s for 20–60 min.

Superoxide Dismutase Activity Assay

The activity of superoxide dismutase (SOD) was determined by using the commercial kit Superoxide Dismutase Activity Assay Kit (Abcam) according to the manufacturer's protocol. The rate of the reduction with a superoxide anion is linearly related to the xanthine

oxidase activity and is inhibited by SOD. Therefore, inhibition activity of SOD was determined by colorimetric method and the absorbance at 450 nm was obtained using SpectraMax M5 microplate reader (Molecular Devices).

Preparation of Macrophages and Stimulation of NLRP3 Inflammasome

Bone marrow-derived macrophages (BMDM) were prepared by isolating bone marrow from the femurs of 8- to 10-week-old C57BL/6 or Nlrp3 KO mice, followed by incubation for 7–10 days with L-cell conditioned medium for macrophage differentiation as we described previously [20]. For NLRP3 inflammasome stimulation, differentiated BMDM were primed with LPS (100 ng/ml) for 1 h and then incubated with nigericin (6.5 μM) for an additional hour [20]. Then, IL-1β-containing conditioned medium (*m*IL-1β-CM) were collected to be added to adipocytes. In some experiments, peritoneal macrophages were used instead of BMDM. For human experiments, human peripheral blood mononuclear cells (*h*PBMC) were purchased from Zenbio and used for *h*IL-1β-CM preparation. *h*PBMC were cultured in RPMI 1640 medium with 10% heat-inactivated FBS, 1% penicillin streptomycin, and 2 mM L-glutamine. Adherent monocyte subpopulations were treated for 5 days with 2 ng/ml of human macrophage colony-stimulating factor (Sigma) for macrophage differentiation. These macrophages then were primed with LPS for 1 h and then exposed to nigericin for 1 h to stimulate NLRP3 inflammasome formation and IL-1β secretion.

Statistical Analysis

All data are presented as mean ± standard error of mean. Independent samples were statistically analyzed using Student's *t* test or one-way ANOVA followed by Tukey's multiple comparison tests for comparisons between two groups. Two-way ANOVA with repeated measures was used to analyze OCR and ROS measurements. All statistical analyses were conducted by Graph Pad Prism 7 (Version 7.03).

RESULTS

TLR4 Activation by LPS Attenuates β3-AR-Induced Thermogenesis

Obesity is associated with high endotoxin level which is a known inducer of TLR4 activation and chronic inflammation. However, inflammation generated by obesity is not as high in amplitude as those seen in acute infectious settings [21, 22]. We reported previously that TLR4 activation by either LPS or a high-fat diet attenuates WAT browning in cold-acclimated mice [13]. Here, we tested whether LPS-induced TLR4 activation could also attenuate β3-AR-induced thermogenesis by using β3-AR-specific agonist (CL 316,243). We found that mice received LPS released less heat in response to β3-AR activation (Fig. 1a, b), induced *Tlr4* gene expression in inguinal sWAT (Fig. 1c), and had higher body weight compared to CL-injected mice (Fig. 1d). LPS-injected group also showed impaired WAT browning in their inguinal fat as brown-like morphology was diminished (Fig. 1e) and the expression of brown-specific genes (*Ucp1*, *Pgc1α*, and *Cidea*) was significantly reduced (Fig. 1f, top), while inflammatory genes (*Tnf-α*, *Il1β*, and *Mcp1*) were elevated (Fig. 1f, bottom) compared to CL-injected mice. These data indicate that TLR4 activation by LPS prevents β3-AR-induced thermogenesis by interfering with WAT browning.

LPS Affects BMP7-Induced Beige Adipogenesis and cAMP-Induced Thermogenesis in Human Adipocytes *In Vitro*

Previously, our group reported that continuous exposure of *h*ASC to BMP7 generates a useful cell model for human beige adipocytes [18]. Using this model, we first tested whether LPS interferes with BMP7-mediated beige adipogenesis. We found that exposure of *h*ASC to LPS along with BMP7 (from the cell expansion before differentiation and throughout differentiation) attenuated BMP7-induced beige adipogenesis as the gene expression of both adipogenic and thermogenic markers all decreased significantly (Fig. 1g). We have also previously reported that exposure of fully differentiated primary human white adipocytes to LPS decreased their thermogenic gene expression in response to Bt_2-cAMP [13]. Here, we next tested the effect of continuous exposure of *h*ASC during adipogenesis to LPS (100 ng/ml) before their exposure to the thermogenic inducer (Bt_2-cAMP).We found that exposure of *h*ASC to LPS markedly decreased adipogenesis and Bt_2-cAMP-induced thermogenic activation, as the gene expression of adipogenic markers (*PPARγ* and *aP2*) and brown-specific markers (*UCP1*, *PGC1a*, *CIDEA*, *DIO2*, and *GLUT4*) reduced significantly (Fig. 1h). These data verify the negative impact of LPS on thermogenesis in two *in vitro* models of human beige adipocytes mediated by BMP7 (Fig. 1f) as well as Bt_2-cAMP (Fig. 1g).

Absence of TLR4 Protects β3-AR-Induced Thermogenesis from the LPS Negative Effects

TLR4 activation inhibited cold-induced thermogenesis, which was rescued in TLR4-mutant mice [13]. In this study, we wanted to verify the role of TLR4 in LPS-induced WAT browning inhibition in response to CL 316,243.We used a genetic model of TLR4-deficient mice and we found that LPS injections in TLR4 KO mice did not cause an increase in body weight (Fig. 2a) as in wild-type mice. In these TLR4 KO mice, LPS did not affect CL-induced WAT browning compared to CL-injected TLR4 KO mice, as both brown-like morphology (Fig. 2b) and brown-specific genes (Fig. 2c) were protected. As expected, the gene expression of inflammatory markers (such as *Tlr4*, *Mcp1*, and *Il1β*) was blunted in these TLR4 KO mice despite LPS administration compared to the wild-type mice (Fig. 2d). We also found that the absence of TLR4 protected mitochondrial content and respiration from the negative effect of LPS (Fig. 2e, f, respectively). These data indicate that LPS-induced inflammation attenuates WAT browning in CL-injected mice *via* TLR4 activation.

TLR4 Activation by LPS Affects Mitochondrial Integrity

Mitochondria play a central role in the metabolism of adipose tissue and adaptive thermogenesis. Therefore, it is not surprising that mitochondrial disruption contributes vastly to impairments in adipose tissue browning [23]. In this study, we tested whether the effect of TLR4 activation on WAT browning involves mitochondrial changes and therefore, we checked mitochondrial morphology, content, and function. We found that mitochondria of inguinal fat cells of LPS+CL-injected mice exhibited atypical morphology, swollen mitochondria with distorted cristae (Fig. 3a). In addition, mitochondrial PCR array indicated abnormal changes in mitochondrial related genes in LPS+CL-injected mice compared to CL group (Fig. 3b). Furthermore, LPS treatment reduced mitochondrial content as determined by mtDNA content in the inguinal fat of CL-injected mice (Fig. 3c). To assess mitochondrial

function, we measured mitochondrial respiration in mouse adipocytes differentiated from C3H10T1/2 pluripotent stem cells. Exposing mature adipocytes to LPS (100 ng/ml) for 24 h reduced mitochondrial respiration significantly (Fig. 3d). To further assess mitochondrial function, we measured mitochondrial membrane potential ($\Delta\psi m$) using a cationic fluorescent dye. Adipocytes treated with LPS caused a 60% elevation in the number of depolarized mitochondria, a reliable indicator of mitochondrial dysfunction (Fig. 3e). Perturbation of the mitochondrial function relates to redox imbalance [23]. Therefore, we measured ROS generation using DCF fluorescence and we found a significant elevation in ROS level in LPS-treated adipocytes (Fig. 3f), which was abrogated upon the antioxidant, n-acetylcysteine (NAC) (Fig. 3g). Furthermore, there was a significant reduction in the SOD enzyme activity (Fig. 3h), which serves to counterbalance the effect of oxidants [24]. Collectively, these results indicate that chronic inflammation induced by TLR4 activation impairs β3-AR-induced browning *via* mechanisms linked to oxidative stress, a convergence outcome of dysfunctional mitochondria and defective antioxidant defense system.

NLRP3 Inflammasome Activation Interferes with Adaptive Thermogenesis

NLR receptors can sense pathogen- and danger-associated molecular patterns [25–27]. A number of obesity-associated danger signals, such as glucose, ceramide, palmitate, and ROS, contribute to NLRP3 inflammasome activation [21, 27]. Activation of NLRP3 inflammasome, during obesity, directly correlates with the severity of diabetes mellitus; however, the role and involvement of obesity-associated NLRP3 inflammasome in adaptive thermogenesis are unknown. Here, we investigated the effect of NLRP3 inflammasome activation in macrophages on Bt_2-cAMP-induced thermogenesis in adipocytes. We stimulated NLRP3 inflammasome by using LPS and nigericin, and then, we collected IL-1β-containing conditioned medium (IL-1β-CM). *IL-1β* gene expression (Fig. 4a, left) induced in human macrophages and IL-1β protein level in the medium also increased significantly upon NLRP3 inflammasome stimulation (Fig. 4a, right). Cultures of primary human adipocytes exposed to *h*IL-1β-CM manifested attenuation in Bt_2-cAMP-induced elevation in *UCP1*, *PGC1α*, *CIDEA*, *and DIO2* (Fig. 4b). In addition, *h*IL-1β-CM attenuated mitochondrial respiration and OCR in these adipocytes (Fig. 4c). To further verify the negative relationship between NLRP3 inflammasome and thermogenesis, we obtained BMDM from wild-type (WT) mice and *Nlrp3*-null mice and we exposed both to same conditions of NLRP3 inflammasome activation. The IL-1β protein content in the obtained media indicates that *Nlrp3*-deficient macrophages had lower ability in IL-1β production compared to WT macrophages (Fig. 4d). Cultures of primary mouse adipocytes incubated with *m*IL-1β-CM derived from WT macrophages showed attenuation in Bt_2-cAMP-induced *Ucp1* gene expression (Fig. 4e, left), while *m*IL-1β-CM derived from NLRP3-deficient macrophages did not affect *Ucp1* gene expression (Fig. 4e, right). Furthermore, there was a dose-dependent effect of *m*IL-1β-CM obtained from WT macrophages on mitochondrial respiration and OCR in adipocytes (Fig. 4f). Area under the curve (AUC) analysis of OCR profile indicates that adipocytes consume more oxygen overall in the absence of *m*IL-1β-CM (Fig. 4f). The ratio of OCR to the extracellular acidification rate (ECAR) may indicate that in the absence of *m*IL-1β-CM, there is a cellular preference of adipocytes for oxidative phosphorylation *versus* glycolysis (Fig. 4f). These data indicate that NLRP3 inflammasome activation in macrophages plays a crucial role in inhibiting white adipocyte browning, and

that targeting NLRP3 inflammasome may break the link between obesity-associated inflammation and impaired adaptive thermogenesis.

IL-1β Mediates the Inhibitory Effect of NLRP3 Inflammasome on Adaptive Thermogenesis

Despite that IL-1β levels are often elevated in obesity and associated with deteriorations in the metabolic functions of multiple organs [6], little is known about the effect of IL-1β on adaptive thermogenesis. In this study, we tested if IL-1β mediates the negative effect of NLRP3 inflammasome on WAT browning. When we blocked IL-1β signaling in adipocytes by using IL-1β receptor antagonist (IL-1RA), UCP1, and other brown-specific markers in human (Fig. 5a) and mouse (Fig. 5b), adipocytes were protected from IL-1β-CM. In addition, IL-1RA improved mitochondrial respiration and OCR compared to adipocytes incubated with IL-1β-CM alone in both human (Fig. 5c) and mouse primary adipocytes (Fig. 5d). Although AUC analysis of OCR profile indicates that IL-1RA improved overall oxygen consumption in adipocytes treated with *m*IL-1β-CM, there was no difference in OCR to ECAR ratio (Fig. 5d). To verify the adverse effects of IL-1β on adaptive thermogenesis, we treated adipocytes directly with IL-1β recombinant protein. There was a dose-dependent effect of IL-1β on the gene expression of brown-specific genes in human adipocytes (Fig. 5e) and animal adipocytes (Fig. 5f). In addition, exposure of adipocytes to IL-1β recombinant protein (20 ng/ml for 24 h) decreased OCR in human adipocytes (Fig. 5g) and animal adipocytes (Fig. 5h). Consistently, the overall oxygen consumption and OCR to ECAR ratio in adipocytes in the presence of IL-1β decreased significantly (Fig. 5h). We also tested the effect of continuous exposure of human adipocytes to IL-1β on BMP7- or Bt_2-cAMP-induced thermogenesis. Combined exposure of adipocytes to BMP7 and IL-1β before and during differentiation inhibited BMP7-induced beige adipocyte development (Supplementary Fig. 1a) and thermogenic genes (Supplementary Fig. 1b). In addition, continuous exposure of adipocytes to IL-1β (2 ng/ml) attenuated adipogenesis (Supplementary Fig. 1c) and blunted Bt_2-cAMP-induced elevation in brown-specific genes (Supplementary Fig. 1d). These data indicate that NLRP3 inflammasome activation in macrophages impose a negative effect on adipocyte browning *via* IL-1β signaling in adipocytes. In addition, exposure of adipocytes to IL-1β affects white and beige adipocyte differentiation and attenuates the gene expression of brown-specific genes.

IL-1β Distresses Mitochondrial Function in Adipocytes

Mitochondrial integrity is crucial for thermogenic program activation [28]. We tested whether IL-1β causes alterations in mitochondrial function and thus interferes with thermogenesis. Using cultures of primary murine adipocytes differentiated from EMSC or sWAT, we found that IL-1β causes a profound increase in ROS production (Fig. 6a). This effect was in a dose-dependent manner (Fig. 6b). Since mitochondria is the major source of ROS, we checked mitochondrial membrane potentials of adipocytes in the presence or absence of IL-1β and we found that IL-1β causes mitochondrial depolarization in a dose-dependent effect (Fig. 6c). To further understand the changes associated with IL-1β-induced ROS elevation, we measured SOD activity and we found that IL-1β decreased SOD activity upon different doses of IL-1β (Fig. 6d). Treating adipocytes with different antioxidants (*i.e.*, NAC or Tempol) resulted in a significant reduction in IL-1β-induced ROS productions (Fig. 6e), protected mitochondrial membrane potential (Fig. 6f), and rescued *Ucp1* gene

expression (Fig. 6g). This suggests that IL-1β in adipocytes intertwines oxidative stress to mitochondrial depolarization through changes in antioxidant defense system; thereby, it inhibits white-to-brown fat conversion.

DISCUSSION

Sustained inflammation exacerbates obesity and metabolic disorders, a state in which non-shivering thermogenesis is reduced. However, the link between inflammation and non-shivering thermogenesis still needs better understanding. In this study, we addressed the question of whether (1) activation of PRR (TLR4 and NLRP3) interferes with β3-AR-induced thermogenesis, (2) the absence of TLR4 and NLRP3 would protect thermogenesis, and (3) whether the pro-inflammatory cytokine, IL-1β, mediates the inhibitory effect of NLRP3 inflammasome on adaptive thermogenesis. Our results demonstrated that LPS-induced TLR4 activation in mice prevented WAT browning despite β3-AR activation, while genetic deletion of TLR4 protected β3-AR-induced thermogenesis. In addition, NLRP3 inflammasome activation in macrophages interfered with Bt_2-cAMP- or norepinephrine-induced thermogenic program in adipocytes, while genetic deletion of NLRP3 in macrophages protected UCP1 gene expression in adipocytes. Furthermore, we found that NLRP3 inflammasome activation in macrophages interfered with thermogenesis of adjacent adipocytes *via* IL-1β paracrine effects, as blocking IL-1 receptor protected adaptive thermogenesis. Finally, we revealed that alterations caused by innate inflammatory system in beige adipocytes were associated with changes in oxidative stress and mitochondrial function. Therefore, our results suggest that anti-inflammatory therapies targeting PRR or inflammatory cytokines may be beneficial for beige fat development.

Activation of PRR, including NLR, plays crucial roles in innate immune responses and inflammation associated with obesity. NLRP3 inflammasome formation requires two signals. The first activating signal involves TLR4 activation to prime the NLRP3 inflammasome leading to induction of pro-caspase-1, pro-IL-1β, and pro-IL-18. The second activating signal involves NLRP3 inflammasome assembly and activation of caspase-1, which then promotes the maturation and release of IL-1β and IL-18 [6, 21, 25, 29, 30]. We found that activation of TLR4 and NLRP3 inflammasome interferes with adaptive thermogenesis. In consistent with our findings, chronic PRR activation was shown to suppress brown adipogenesis of multipotent mesodermal stem cells and brown pre-adipocytes [31]. As activation of NLRP3 inflammasome results in IL-1β production, we found that IL-1β mediates the abrogation in adaptive thermogenesis caused by NLRP3 inflammasome in our study. Our data are consistent with the previous report in which IL-1β was found to be potent in suppressing isoproterenol-induced UCP-1 mRNA expression in adipocytes [1, 15].

Mitochondria constitute the primary source of ROS generation. ROS function as physiological signaling molecules; however, prolonged and excessive ROS could be damaging to the cells, leading to different pathological changes [24]. We found that low amplitude of inflammation in adipocytes by TLR4 (Fig. 3f) or IL-1R (Fig. 6a, b) activation results in high levels of ROS production. In addition, the enzyme activity of SOD, an important enzymatic scavenger of antioxidant defense [24], is abrogated by LPS (Fig. 3h)

and IL-1β (Fig. 6d). The changes in oxidative stress status in adipocytes were associated with an elevation in mitochondrial depolarization upon the treatments with LPS (Fig. 3e) or IL-1β (Fig. 6c), while mitochondrial depolarization was reduced in the presence of antioxidants (Fig. 6f). This implicates an intertwined relationship between oxidative stress and mitochondrial function in adipocytes under inflammation. We, therefore, find it plausible that chronic inflammation in adipocytes shifts the cellular redox balance and that oxidative stress in combination with mitochondrial damage underlies the impairment in browning potentials.

Depending on the state of the adipose tissue, lean or obese, the immune cells could be changed dynamically. Macrophages have the potential to express both anti- and pro-inflammatory cytokines. Some reports focus on the positive role of anti-inflammatory cytokines in adipocyte beigeing [4, 32], while others focus on the negative role of pro-inflammatory cytokines [13, 31, 32]. Modulation of the innate immune system and inflammation in improving energy dissipation is still not entirely understood and, in humans, has yet to be demonstrated. Dedicated experiments are especially needed for clarifying the regulatory role of the complex interplay between anti- and pro-inflammatory system in adaptive thermogenesis, and whether activation of anti-inflammatory system can override the inhibitory effect of the pro-inflammatory system.

Some evidence indicates that classical brown adipocytes are less prone to inflammation and this may be linked to their thermogenic potentials. The reduced inflammation in the interscapular brown adipose tissue (iBAT) may be a key factor in its thermogenic nature. In one study, macrophage infiltration and inflammatory cytokines expression in iBAT were reported to be significantly less than that in WAT in diet-induced obese (DIO) mice and normal mice [33]. Also, brown adipocytes were reported to have an ability in suppressing inflammatory genes in macrophages compared to white adipocytes [33]. These experiments provide another evidence for the inverse relationship between inflammatory cytokines and non-shivering thermogenesis, emphasizing on the importance of suppressing inflammation to promote adaptive thermogenesis.

Although we attributed dysfunctional WAT browning to the chronic inflammatory responses associated with obesity, several other obesity-associated factors might play a key role in dysfunctional WAT browning. For instance, the transforming growth factor β (TGF β) and Notch signaling pathways were shown to react as negative regulators of thermogenesis in obese mice [34]. Furthermore, autophagy was found to dysregulate beige adipogenesis, as inhibiting autophagy through deletion of Atg7 in adipocytes led to increased beige adipocyte differentiation in DIO mice [35, 36]. Our group also has observed that autophagy profoundly contributes to LPS-induced beige fat inhibition [13]. Therefore, revealing the cross-talk between inflammation and these factors in adaptive thermogenesis will provide indispensable knowledge for identifying therapeutic targets for promoting energy dissipation and preventing obesity.

CONCLUSION

The revived interest in targeting BAT in adults to promote energy expenditure with subsequent decreases in adiposity instigates our needs for better understanding of the metabolic circuit of immune system in beige adipocyte recruitment to activate non-shivering thermogenesis. We view obesity as a deregulator of beige adipocyte development due to its associated chronic immune responses. We found that inflammation interferes with metabolic adaption to β3-AR-induced WAT browning *via* mechanisms linked to oxidative stress and mitochondrial dysfunction. Thus, therapeutic strategies aiming to stimulate non-shivering thermogenesis to protect against obesity may become efficient if accompanied by those targeting inflammatory burden or oxidative stress in the fat tissue.

Supplementary Material

Refer to Web version on PubMed Central for supplementary material.

Acknowledgments

The authors wish to acknowledge the College of Medicine Research Center (CMRC) at King Saud University (KSU) and the Stem cell lab in the College of Medicine at KSU for providing access to their facilities to perform mitochondrial depolarization and oxidative stress experiments. Also, the authors wish to thank Rabih Halwani at the College of Medicine in KSU for permitting the use of Muse flow cytometry.

Funding This study was supported by the National Institute of Health (Grant 1P20GM104320, project 5; to S. C.) in the USA, International Scientific Partnership Program (ISPP, no. 0103) at King Saud University (KSU) in Saudi Arabia, and Deanship of Scientific Research (Project No. R6-17-02-36) at King Saud University in Saudi Arabia.

Abbreviations

NLRP3	NOD-like receptor protein 3
TLR4	Toll-like receptor 4
WAT	White adipose tissue
PRR	pattern recognition receptors
β3-AR	beta 3-adrenergic receptor
ROS	reactive oxygen species
UCP1	uncoupling protein 1
IL1β	interleukin-1 beta
BMP7	bone morphogenetic protein 7
LPS	lipopolysaccharide
CL	CL 316,243
hASCs	human adipose-derived stem cells
EMSC	ear mesenchymal stem cells

sWAT	subcutaneous white adipose tissue
mtDNA	mitochondrial DNA
OCR	oxygen consumption rate
SOD	superoxide dismutase
hIL1β-CM	human interleukin-1 beta-conditioned medium
mIL1β-CM	mouse interleukin-1 beta-conditioned medium
NAC	n-acetylcysteine
Bt2-cAMP	dibutyryl-cAMP
IL1RA	IL1 receptor antagonist
MQ	macrophages

References

1. Alexaki VI, Chavakis T. The role of innate immunity in the regulation of brown and beige adipogenesis. Reviews in endocrine & metabolic disorders. 2016; 17(1):41–49. [PubMed: 26910560]
2. Reitman ML. How does fat transition from white to beige? Cell metabolism. 2017; 26(1):14–16. [PubMed: 28683281]
3. Qiu Y, Nguyen KD, Odegaard JI, Cui X, Tian X, Locksley RM, et al. Eosinophils and type 2 cytokine signaling in macrophages orchestrate development of functional beige fat. Cell. 2014; 157(6):1292–1308. [PubMed: 24906148]
4. Nguyen KD, Qiu Y, Cui X, Goh YP, Mwangi J, David T, et al. Alternatively activated macrophages produce catecholamines to sustain adaptive thermogenesis. Nature. 2011; 480(7375):104–108. [PubMed: 22101429]
5. Chmelar J, Chung KJ, Chavakis T. The role of innate immune cells in obese adipose tissue inflammation and development of insulin resistance. Thrombosis and haemostasis. 2013; 109(3): 399–406. [PubMed: 23364297]
6. Lackey DE, Olefsky JM. Regulation of metabolism by the innate immune system. Nature reviews Endocrinology. 2016; 12(1):15–28.
7. Thyagarajan B, Foster MT. Beiging of white adipose tissue as a therapeutic strategy for weight loss in humans. Hormone molecular biology and clinical investigation. 2017
8. van Marken Lichtenbelt WD, Vanhommerig JW, Smulders NM, Drossaerts JM, Kemerink GJ, Bouvy ND, et al. Cold-activated brown adipose tissue in healthy men. The New England Journal of Medicine. 2009; 360(15):1500–1508. [PubMed: 19357405]
9. Saito M, Okamatsu-Ogura Y, Matsushita M, Watanabe K, Yoneshiro T, Nio-Kobayashi J, et al. High incidence of metabolically active brown adipose tissue in healthy adult humans: effects of cold exposure and adiposity. Diabetes. 2009; 58(7):1526–1531. [PubMed: 19401428]
10. Vijgen GH, Bouvy ND, Teule GJ, Brans B, Schrauwen P, van Marken Lichtenbelt WD. Brown adipose tissue in morbidly obese subjects. PLoS One. 2011; 6(2):e17247. [PubMed: 21390318]
11. Cypess AM, Lehman S, Williams G, Tal I, Rodman D, Goldfine AB, et al. Identification and importance of brown adipose tissue in adult humans. The New England journal of medicine. 2009; 360(15):1509–1517. [PubMed: 19357406]
12. Martins FF, Bargut TCL, Aguila MB, Mandarim-de-Lacerda CA. Thermogenesis, fatty acid synthesis with oxidation, and inflammation in the brown adipose tissue of ob/ob (−/−) mice. Annals of anatomy. Anatomischer Anzeiger : official organ of the Anatomische Gesellschaft. 2017; 210:44–51.

13. Okla M, Wang W, Kang I, Pashaj A, Carr T, Chung S. Activation of Toll-like receptor 4 (TLR4) attenuates adaptive thermogenesis via endoplasmic reticulum stress. The Journal of Biological Chemistry. 2015; 290(44):26476–26490. [PubMed: 26370079]
14. Lumeng CN, Bodzin JL, Saltiel AR. Obesity induces a phenotypic switch in adipose tissue macrophage polarization. The Journal of Clinical Investigation. 2007; 117(1):175–184. [PubMed: 17200717]
15. Sakamoto T, Takahashi N, Sawaragi Y, Naknukool S, Yu R, Goto T, et al. Inflammation induced by RAW macrophages suppresses UCP1 mRNA induction via ERK activation in 10T1/2 adipocytes. American Journal of Physiology Cell Physiology. 2013; 304(8):C729–C738. [PubMed: 23302779]
16. Goto T, Naknukool S, Yoshitake R, Hanafusa Y, Tokiwa S, Li Y, et al. Proinflammatory cytokine interleukin-1beta suppresses cold-induced thermogenesis in adipocytes. Cytokine. 2016; 77:107–114. [PubMed: 26556104]
17. Crane JD, Mottillo EP, Farncombe TH, Morrison KM, Steinberg GR. A standardized infrared imaging technique that specifically detects UCP1-mediated thermogenesis in vivo. Molecular Metabolism. 2014; 3(4):490–494. [PubMed: 24944909]
18. Okla M, Ha JH, Temel RE, Chung S. BMP7 drives human adipogenic stem cells into metabolically active beige adipocytes. Lipids. 2015; 50(2):111–120. [PubMed: 25534037]
19. Kim J, Okla M, Erickson A, Carr T, Natarajan SK, Chung S. Eicosapentaenoic acid potentiates brown thermogenesis through FFAR4-dependent up-regulation of miR-30b and miR-378. The Journal of Biological Chemistry. 2016; 291(39):20551–20562. [PubMed: 27489163]
20. Kim Y, Wang W, Okla M, Kang I, Moreau R, Chung S. Suppression of NLRP3 inflammasome by gamma-tocotrienol ameliorates type 2 diabetes. Journal of Lipid Research. 2016; 57(1):66–76. [PubMed: 26628639]
21. Lumeng CN. Innate immune activation in obesity. Molecular Aspects of Medicine. 2013; 34(1): 12–29. [PubMed: 23068074]
22. Hotamisligil GS. Inflammation and metabolic disorders. Nature. 2006; 444(7121):860–867. [PubMed: 17167474]
23. Pelicano H, Lu W, Zhou Y, Zhang W, Chen Z, Hu Y, et al. Mitochondrial dysfunction and reactive oxygen species imbalance promote breast cancer cell motility through a CXCL14-mediated mechanism. Cancer Research. 2009; 69(6):2375–2383. [PubMed: 19276362]
24. Birben E, Sahiner UM, Sackesen C, Erzurum S, Kalayci O. Oxidative stress and antioxidant defense. The World Allergy Organization Journal. 2012; 5(1):9–19. [PubMed: 23268465]
25. Vandanmagsar B, Youm YH, Ravussin A, Galgani JE, Stadler K, Mynatt RL, et al. The NLRP3 inflammasome instigates obesity-induced inflammation and insulin resistance. Nature Medicine. 2011; 17(2):179–188.
26. Tack CJ, Stienstra R, Joosten LA, Netea MG. Inflammation links excess fat to insulin resistance: the role of the interleukin-1 family. Immunological Reviews. 2012; 249(1):239–252. [PubMed: 22889226]
27. Wen H, Gris D, Lei Y, Jha S, Zhang L, Huang MT, et al. Fatty acid-induced NLRP3-ASC inflammasome activation interferes with insulin signaling. Nature Immunology. 2011; 12(5):408–415. [PubMed: 21478880]
28. Cedikova M, Kripnerova M, Dvorakova J, Pitule P, Grundmanova M, Babuska V, et al. Mitochondria in white, brown, and beige adipocytes. Stem cells International. 2016; 2016:6067349. [PubMed: 27073398]
29. Stienstra R, Tack CJ, Kanneganti TD, Joosten LA, Netea MG. The inflammasome puts obesity in the danger zone. Cell Metabolism. 2012; 15(1):10–18. [PubMed: 22225872]
30. Benetti E, Chiazza F, Patel NS, Collino M. The NLRP3 Inflammasome as a novel player of the intercellular crosstalk in metabolic disorders. Mediators of Inflammation. 2013; 2013:678627. [PubMed: 23843683]
31. Bae J, Chen J, Zhao L. Chronic activation of pattern recognition receptors suppresses brown adipogenesis of multipotent mesodermal stem cells and brown pre-adipocytes. Biochemistry and cell biology = Biochimie et biologie cellulaire. 2015; 93(3):251–261. [PubMed: 25741603]

32. Finlin BS, Zhu B, Confides AL, Westgate PM, Harfmann BD, Dupont-Versteegden EE, et al. Mast cells promote seasonal white adipose beiging in humans. Diabetes. 2017; 66(5):1237–1246. [PubMed: 28250021]

33. Dowal L, Parameswaran P, Phat S, Akella S, Majumdar ID, Ranjan J, et al. Intrinsic properties of brown and white adipocytes have differential effects on macrophage inflammatory responses. Mediators of Inflammation. 2017; 2017:9067049. [PubMed: 28458470]

34. Bi P, Shan T, Liu W, Yue F, Yang X, Liang XR, et al. Inhibition of Notch signaling promotes browning of white adipose tissue and ameliorates obesity. Nature Medicine. 2014; 20(8):911–918.

35. Altshuler-Keylin S, Kajimura S. Mitochondrial homeostasis in adipose tissue remodeling. Science signaling. 2017; 10(468)

36. Zhang Y, Goldman S, Baerga R, Zhao Y, Komatsu M, Jin S. Adipose-specific deletion of autophagy-related gene 7 (atg7) in mice reveals a role in adipogenesis. Proceedings of the National Academy of Sciences of the United States of America. 2009; 106(47):19860–19865. [PubMed: 19910529]

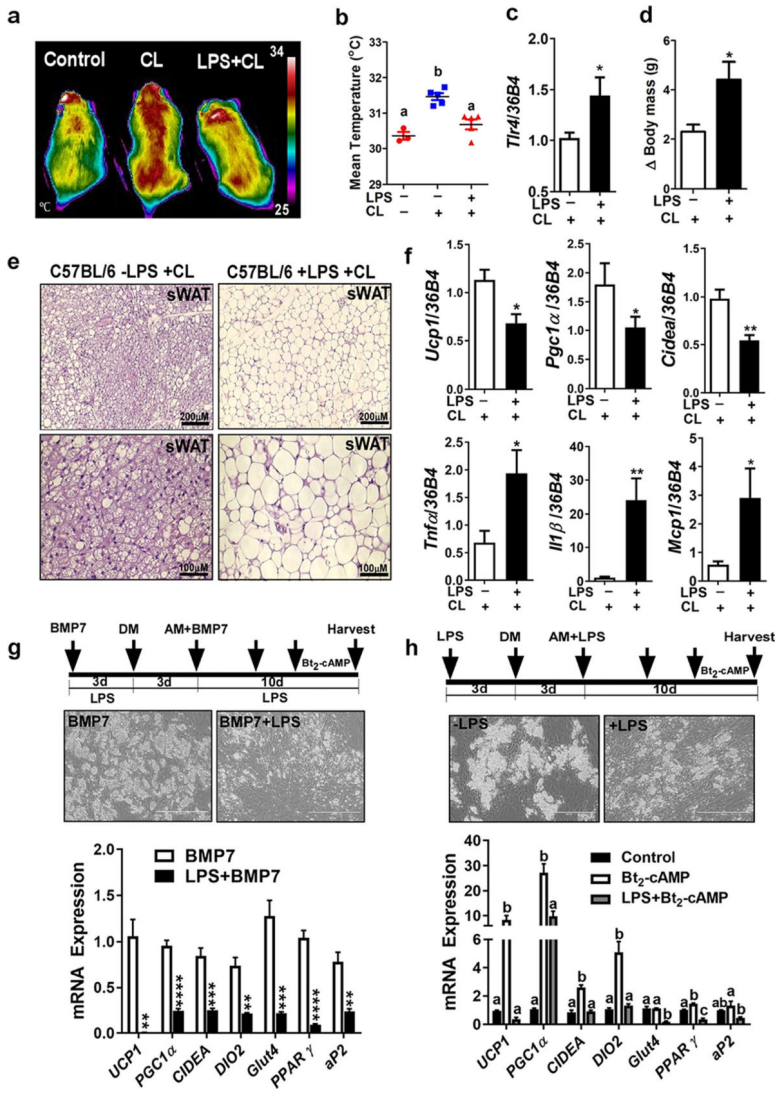

Fig. 1.

LPS-induced TLR4 activation attenuates β3AR-induced thermogenesis and prevents WAT browning. **a**–**f** C57BL/6 male mice received i.p. injections of either saline (control), CL, or LPS+CL as described in experimental procedures (n = 6–8). **a** Representative thermography captured by IR camera. **b** Mean surface body temperature recorded by IR camera. **c** Relative *Tlr4* mRNA level in inguinal sWAT. **d** Body weight changes over the course of administering either CL or LPS+CL. **e** Representative microscopic images of H&E staining for sWAT (scale bar = 100 μm). **f** Relative gene expression analysis by qPCR of sWAT. **g** *h*ASC exposed to BMP7-conditioned medium in the presence or absence of LPS (100 ng/ml before and during adipocyte differentiation), and followed by Bt_2-cAMP (0.5mM) stimulation for 7 h before harvesting mRNA. **g** and **h** Cultures of primary human adipocytes differentiated from human adipose-derived stem cells (*h*ASC) as explained in experimental procedures. **g** (top panel) Phase contrast images for adipocytes 10 days after differentiation (scale bar = 400 μm). Arrows indicate the time line for LPS and BMP7 addition and initiation of adipocyte differentiation by adding differentiation medium (DM) and adipocyte

maintenance medium (AM). **g** (bottom panel) Relative gene expression analysis by qPCR. **h** *h*ASC exposed to LPS (100 ng/ml) before and during differentiation, and followed by Bt_2-cAMP (0.5 mM) stimulation for 7 h before harvesting mRNA. **h** (top panel) Phase contrast images for adipocytes 10 days after differentiation (scale bar = 400 μm). Arrows indicate the time line for LPS addition and initiation of adipocyte differentiation (DM) and maintenance (AM). **h** (bottom panel) Relative gene expression analysis by qPCR. All data are presented as mean ± SEM. *$P < 0.05$, **$P < 0.01$, ***$P < 0.001$, and ****$P < 0.0001$ by Student's *t* test. Values not sharing a common letter differ significantly ($P < 0.05$) by one-way ANOVA. *sWAT*, subcutaneous white adipose tissue; *CL*, CL-316,243; *LPS*, lipopolysaccharides; *BMP7*, bone morphogenic protein; *UCP1*, uncoupling protein 1; *PGC1α*, peroxisome proliferator-activated receptor gamma coactivator 1-alpha; *CIDEA*, cell death-inducing DFFA-like effector A; *TNF-α*, tumor necrosis factor-alpha; *IL-1β*, interleukin-1 beta; *MCP1*, monocyte chemoattractant protein-1.

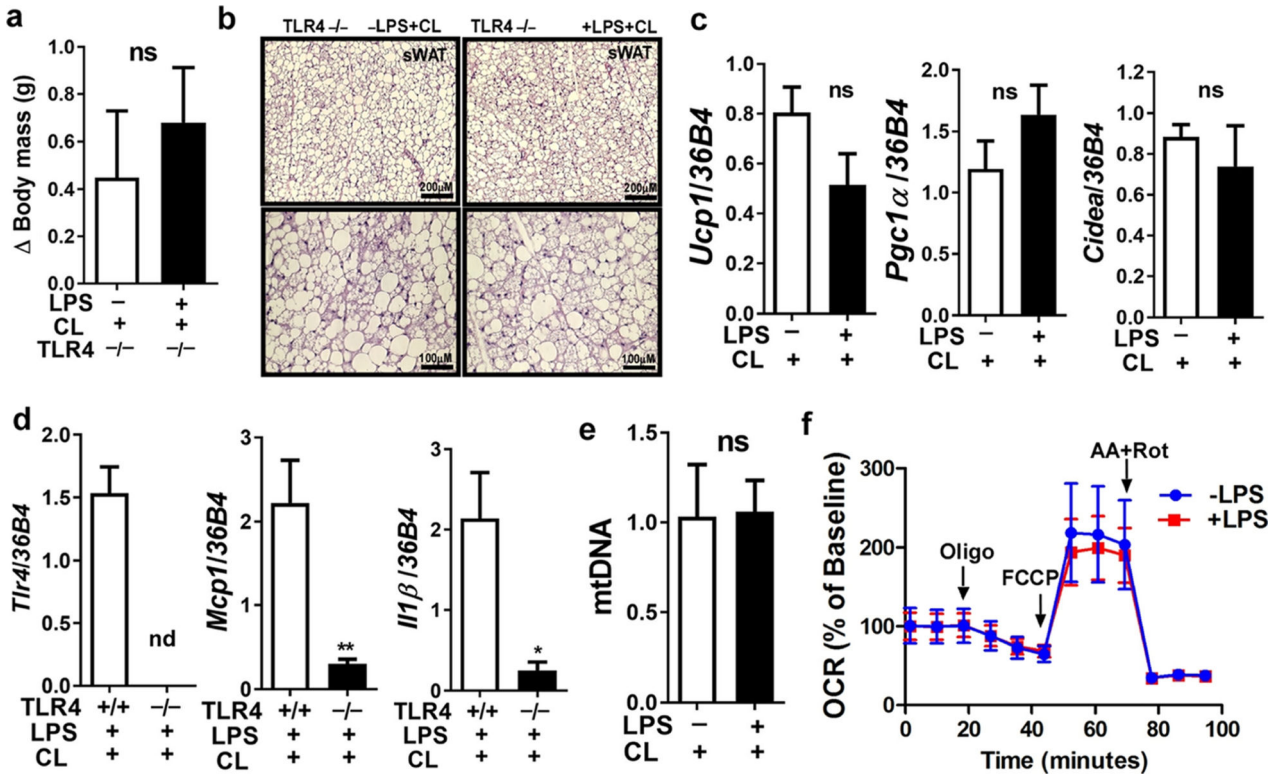

Fig. 2.

Absence of TLR4 protects from the influence of LPS on adaptive thermogenesis, WAT browning, and mitochondrial integrity. **a** Body weight changes over the course of administering either CL or LPS+CL to the *Tlr4*-null male mice ($n = 6–8$). **b** Representative images of H&E staining for sWAT of TLR4 KO mice (scale bar = 100 μm). **c** and **d** Relative gene expression analysis by qPCR of sWAT obtained from TLR4 KO mice received either CL or LPS+CL. **e** Relative mtDNA contents in axillary sWAT of LPS and LPS+CL-injected TLR4 KO mice. **f** OCR measurements by Seahorse extracellular analyzer for TLR4-deficient primary mouse adipocytes differentiated from subcutaneous fat-derived stem cell from TLR-deficient male mice, and treated with either vehicle or LPS. Arrow indicates the addition of respiratory inhibitors of oligomycin (Oligo), FCCP, and rotenone plus antimycin A (Rot+AA) (two-way ANOVA, $P > 0.05$). All data are presented as mean ± SEM. $^{*}P < 0.05$ and $^{**}P < 0.01$ by Student's *t* test. *ns*, not significant; *nd*, not detected.

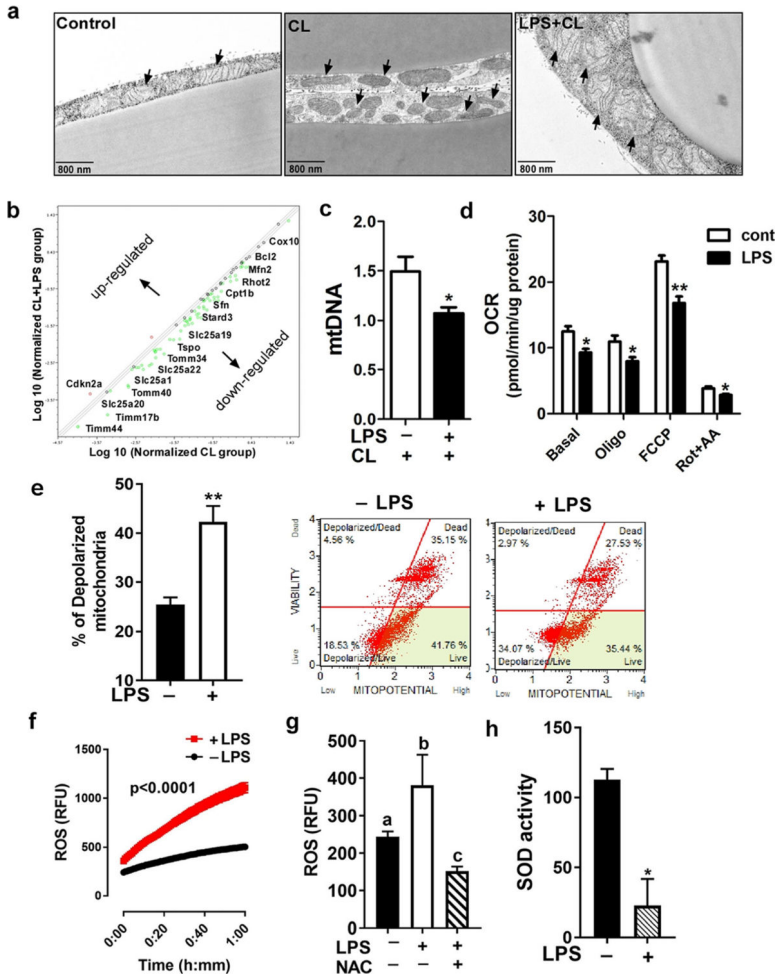

Fig. 3.

TLR4 activation affects mitochondrial morphology, content, and function. **a** Transmission electron microscopic images of inguinal sWAT of C57BL/6 male mice received either saline (control), CL, or LPS+CL as described in experimental procedures. Arrows indicate mitochondria. **b** Microarray analysis of mouse mitochondrial genes (84 genes) by qPCR as described in experimental procedures for inguinal sWAT of C57BL/6 male mice using pooled mRNA for 6–8 mice. Broken lines indicate twofold expression of differences between treatments. **c** Relative mtDNA contents in axillary sWAT of LPS and LPS+CL-injected mice, **d** Seahorse analysis of OCR in mouse C3H10T1/2 adipocytes treated with or without LPS (100 ng/ml for 24 h) as described in experimental procedures. **e** Analysis of depolarized mitochondria as obtained by the Muse flow cytometer using primary mouse adipocytes differentiated from subcutaneous fat-derived stem cells of C57BL/6 male mice, and treated with or without LPS (100 ng/ml) as described in experimental procedures. **e** (left) The graph represents the percentage of total depolarized cells. **e** (right) Representative scattered plots showing the percentages of live and dead depolarized cells. **f** ROS levels as detected by DCF fluorescence in primary mouse adipocytes differentiated from ear mesenchymal stem cells (EMSC) of C57BL/6 male mice (two-way ANOVA, $P < 0.0001$). **g** ROS levels produced in EMSC-derived mouse adipocytes in the presence or absence of LPS

and NAC. **h** SOD enzyme activity in EMSC-derived mouse adipocytes as described in experimental procedures. All data are presented as mean ± SEM. $*P < 0.05$ and $**P < 0.01$ by Student's *t* test. Values not sharing a common letter differ significantly ($P < 0.05$) by one-way ANOVA. *mtDNA*, mitochondrial DNA; *OCR*, oxygen consumption rate; *ROS*, reactive oxygen species; *NAC*, n-acetylcysteine; *SOD*, superoxide dismutase.

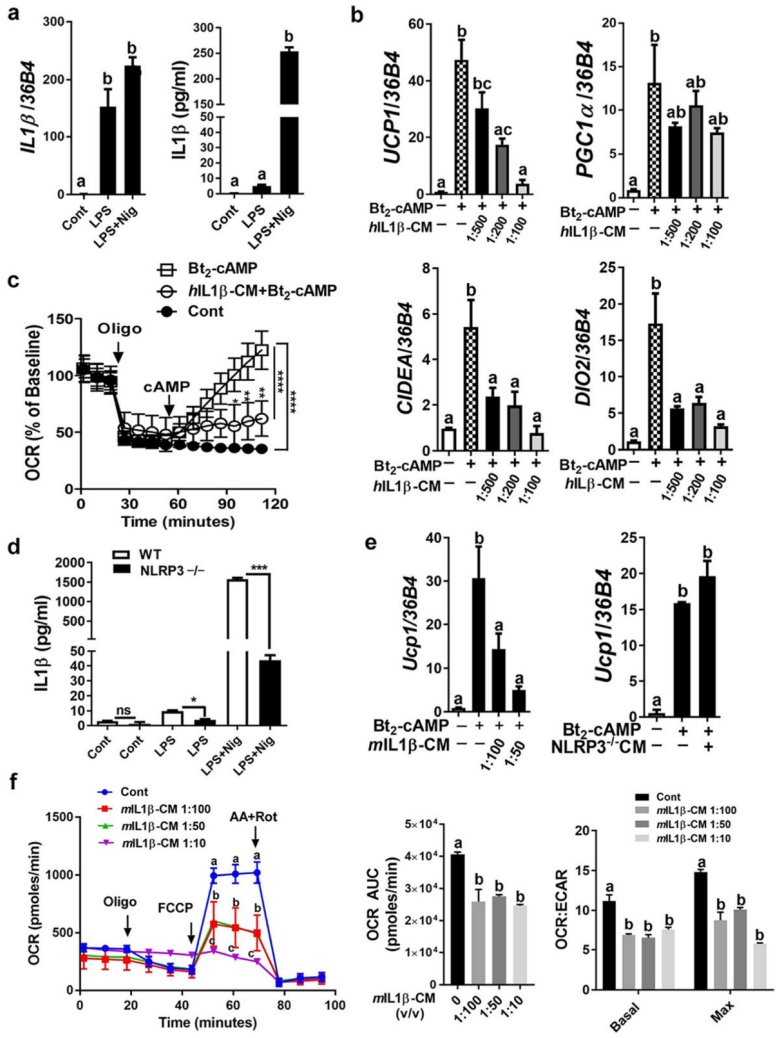

Fig. 4.

NLRP3 inflammasome attenuates browning of human and mouse primary adipocytes. **a** Inflammasome activation was triggered by LPS and nigericin in *h*PBMC as described in experimental procedures. Relative *IL-1β* mRNA level (left) was measured by qPCR and IL-1β secretion (in medium) (right) was quantified by ELISA. **b** Relative mRNA level of *UCP1* and *PGC1α* in primary cultures of human adipocytes incubated with different doses of *h*IL-1β-CM for 12 h before stimulating with Bt_2-cAMP (0.7 mM for 7 h). **c** OCR obtained by Seahorse extracellular analyzer for human adipocytes pre-incubated with either control (conditioned medium obtained from unstimulated macrophages) or *h*IL-1β-CM (1:100 for 24 h). Arrow indicates the addition of oligomycin (Oligo) and Bt_2-cAMP (two-way ANOVA, $*P < 0.05$, $**P < 0.001$, $****P < 0.0001$). **d** ELISA quantification of IL-1β in the medium obtained from BMDM of WT or NLRP3 KO mice. The BMDM were stimulated with vehicle, LPS alone, or LPS plus nigericin. **e** Relative gene expression of *Ucp1* in mouse adipocytes differentiated from EMSC of C57BL/6 male mice and incubated with either *m*IL-1β-CM obtained from wild-type (WT) MQ (left) or NLRP3 KO MQ (right) and then stimulated with Bt_2-cAMP. **f** OCR Seahorse profiles with AUC analysis and OCR:ECAR ratio at either basal or maximal respiration for mouse adipocytes differentiated

from EMSC of WT mice, and treated with different doses of *m*IL-1β-CM from WT MQ (two-way ANOVA, values not sharing a common letter differ significantly, $P < 0.05$). All data are presented as mean ± SEM. *$P < 0.05$, **$P < 0.01$, and ***$P < 0.001$ by Student's *t* test. Values not sharing a common letter differ significantly ($P < 0.05$) by one-way ANOVA. *AUC*, area under the curve; *ECAR*, extracellular acidification rate.

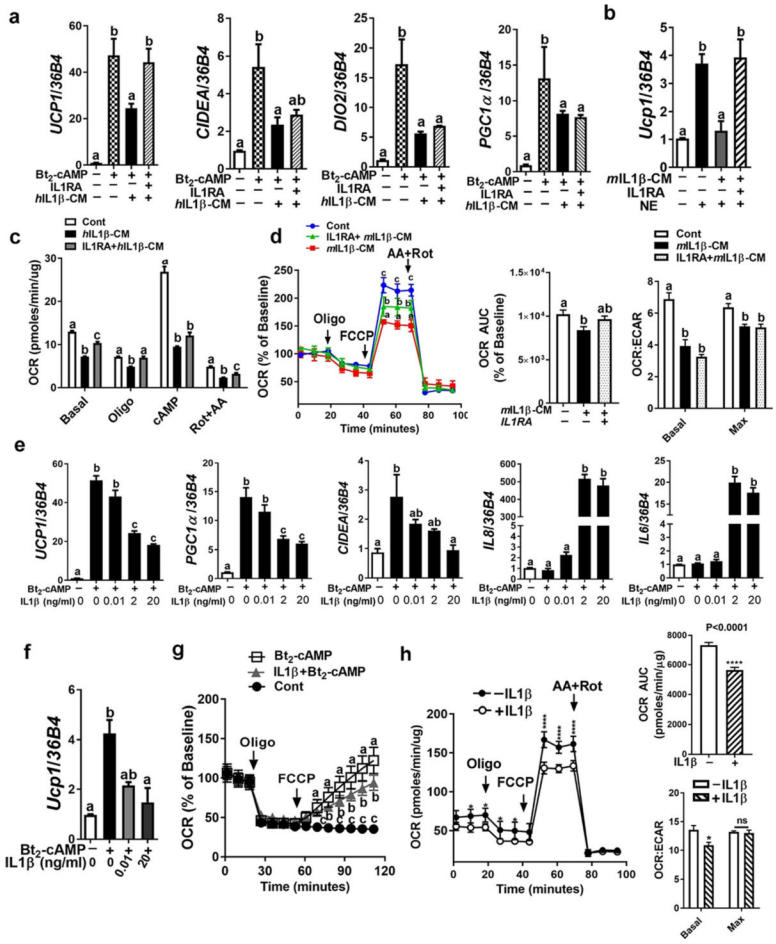

Fig. 5.

IL-1β mediates the inhibitory effect of NLRP3 inflammasome on thermogenesis. **a** Relative gene expression of *UCP1*, *CIDEA*, *PGC1α*, and *DIO2* by qPCR for primary cultures of human adipocytes pre-treated with IL-1β receptor antagonist (IL-1RA) (30 μM for 1 h), incubated with *h*IL-1β-CM (1:500 for 24 h), and then stimulated with Bt_2-cAMP (0.7 mM for 8 h). **b** mRNA level of *Ucp1* by qPCR for C3H10T1/2 mouse adipocytes pre-treated with IL-1RA (10 μM for 1 h), incubated with *m*IL-1β-CM (1:100 for 12 h), and after that stimulated with NE (10 μM for 4 h). **c** OCR by Seahorse extracellular analyzer for human adipocytes pre-treated with IL-1RA and then treated with *h*IL-1β-CM (one-way ANOVA, values not sharing a common letter in each stage of respiration differ significantly, $P < 0.05$). **d** OCR Seahorse profiles with AUC analysis and OCR to ECAR ratio at either basal or maximal respiration for C3H10T1/2 mouse adipocytes pre-treated with IL-1RA and then incubated with *m*IL-1β-CM. Arrow indicates the addition of respiratory inhibitors of oligomycin (Oligo), FCCP, and rotenone plus antimycin A (Rot+AA) (two-way ANOVA, values not sharing a common letter differ significantly, $P < 0.05$). **e** mRNA levels of thermogenic and inflammatory genes for human adipocytes treated with different doses of human recombinant IL-1β protein. **f** *Ucp1* mRNA level upon treatments of C3H10T1/2 mouse adipocytes with different doses of mouse recombinant IL-1β protein. **g** OCR by Seahorse extracellular analyzer for human adipocytes incubated with IL-1β recombinant

protein (20 ng/ml for 24 h) (two-way ANOVA, values not sharing a common letter differ significantly, $P < 0.05$). **h** OCR Seahorse profiles with AUC analysis and OCR to ECAR ratio at either basal or maximal respiration for C3H10T1/2 mouse adipocytes in the presence or absence of IL-1β recombinant protein (2 ng/ml for 24 h) (two-way ANOVA, $*P < 0.05$, $****P < 0.0001$). All data are presented as mean ± SEM. $*P < 0.05$, $**P < 0.01$, and $***P < 0.001$ by Student's *t* test. Values not sharing a common letter differ significantly ($P < 0.05$) by one-way ANOVA.

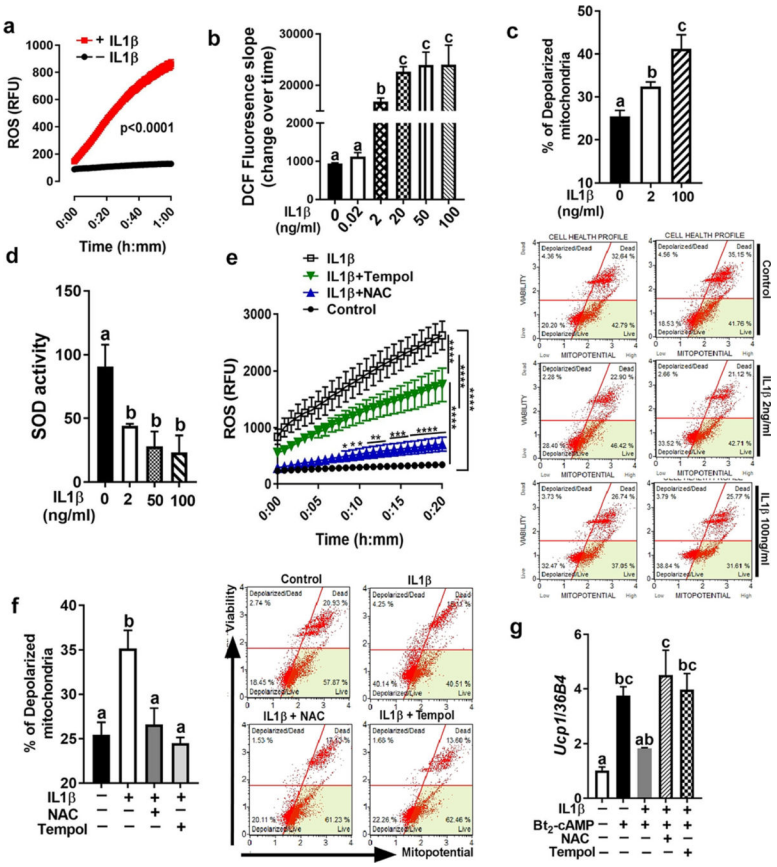

Fig. 6.

IL-1β stimulates oxidative stress and affects mitochondrial membrane potential. **a** ROS production in primary mouse adipocytes differentiated from EMSC of C57BL/6 male mice, and incubated with or with IL-1β (2 ng/ml for 48 h) as determined by DCF fluorescence (two-way ANOVA, $P < 0.0001$). **b** ROS production in mouse adipocytes differentiated from EMSC, and treated with different doses of IL-1β. **c** Percentage of total depolarized mitochondria in mouse adipocytes differentiated from subcutaneous fat of C57BL/6 male mice, and treated with different doses of IL-1β (for 24 h) as measured by Muse flow cytometer. **c** (top panel) The graph represents the percentage of total depolarized cells. **c** (bottom panel) Representative scattered plots showing the percentages of live and dead depolarized cells. **d** SOD enzyme activity in mouse adipocytes differentiated from subcutaneous fat of C57BL/6 male mice, and stimulated with different doses of IL-1β (for 48 h). **e** ROS production in mouse adipocytes differentiated from EMSC of C57BL/6 male mice, and treated with antioxidants (either 200 μM NAC or 100 μM Tempol) along with IL-1β (2 ng/ml for 24 h) (two-way ANOVA, $*P < 0.05$, $**P < 0.001$, $****P < 0.0001$). **f** Mitochondrial membrane potential measured by Muse flow cytometer in mouse adipocytes differentiated from subcutaneous fat of C57BL/6 male mice, and exposed to antioxidants (either 200 μM NAC or 100 μM Tempol) along with IL-1β (2 ng/ml for 24 h). **f** (left) The graph represents the percentage of total depolarized cells. **f** (right) Representative scattered plots showing the percentages of live and dead depolarized cells. **g** *Ucp1* mRNA levels in primary mouse adipocytes differentiated from EMSC of C57BL/6 male mice, and treated

with either NAC (200 μM) or Tempol (200 μM) along with IL-1β (2 ng/ml for 24 h) as determined by qPCR. All data are presented as mean ± SEM. Values not sharing a common letter differ significantly ($P < 0.05$) by one-way ANOVA.

Supplementary Material

Inhibitory effects of Toll-like receptor 4, NLRP3 inflammasome, and interleukin-1β on white adipocyte browning

Meshail Okla[1,2,*], Walid Zaher[3,4], Musaad Alfayez[5], Soonkyu Chung[1]

[1] Department of Nutrition and Health Sciences, University of Nebraska-Lincoln, Lincoln, NE, United States

[2] Department of Community Health Sciences, College of Applied Medical Sciences, King Saud University, Riyadh, Saudi Arabia

[3] College of Medicine Research Center, College of Medicine, King Saud University, Riyadh, Saudi Arabia

[4] Department of Anatomy, College of Medicine, King Saud University, Riyadh, Saudi Arabia

[5] Stem Cell Unit, Department of Anatomy, College of Medicine, King Saud University, Riyadh, Saudi Arabia

[*]To whom correspondence should be addressed: Meshail Okla, Ph.D., Department of Community Health Sciences, College of Applied Medical Sciences, King Saud University, 183T11, P.O. Box 22452, Riyadh, Saudi Arabia, 11495, Tel: +966 11 80 58 401, E-mail address: meokla@ksu.edu.sa

Supplementary Table 1. List of real-time PCR primer sequences

Gene	Forward (5'→3')	Reverse (5'→3')
m36B4	GGATCTGCTGCATCTGCTTG	GGCGACCTGGAAGTCCAACT
mUCP1	AGGCTTCCAGTACCATTAGGT	CTGAGTGAGGCAAAGCTGATTT
mPGC1α	CCCTGCCATTGTTAAGACC	TGCTGCTGTTCCTGTTTTC
mCIDEA	TGCTCTTCTGTATCGCCCAGT	GCCGTGTTAAGGAATCTGCTG
mTNFα	GGCTGCCCCGACTACGT	ACTTTCTCCTGGTATGAGATAGCAAAT
mIL1β	GTCACAAGAAACCATGGCACAT	GCCCATCAGAGGCAAGGA
mMCP1	AGGTCCCTGTCATGCTTCTG	GCTGCTGGTGATCCTCTTGT
h36B4	GAAGGCTGTGGTGCTGATG	GTGAGGTCCTCCTTGGTGAA
hUCP1	TCTCTCAGGATCGGCCTCTA	GTGGGTTGCCCAATGAATAC
hPGC1a	GTGAAGACCAGCCTCTTTGC	TCACTGCACCACTTGAGTCC
hCIDEA	CTTAACGTGAAGGCCACCAT	AGAAACTGTCCCGTCACCTG
hDIO2	CCTCCTCGATGCCTACAAAC	GCTGGCAAAGTCAAGAAGGT
hGLUT4	GCTACCTCTACATCATCCAGAATCTC	CCAGAAACATCGGCCCA
hPPARγ	AGCCTCATGAAGAGCCTTCCA	TCCGGAAGAAACCCTTGCA
haP2	ACTGGGCCAGGAATTTGACGAAGT	TCTCGTGGAAGTGACGCCTTTCAT
hIL1β	GCCCTAAACAGATGAAGTGCTC	GAACCAGCATCTTCCTCA
hIL8	GCT CTG TGT GAA GGT GCA GTT	AAT TTC TGT GTT GGC GCA GT
hIL6	CTT CTC CAC AAG CGC CTT C	CAG GCA ACA CCA GGA GCA

Supplementary Fig. 1

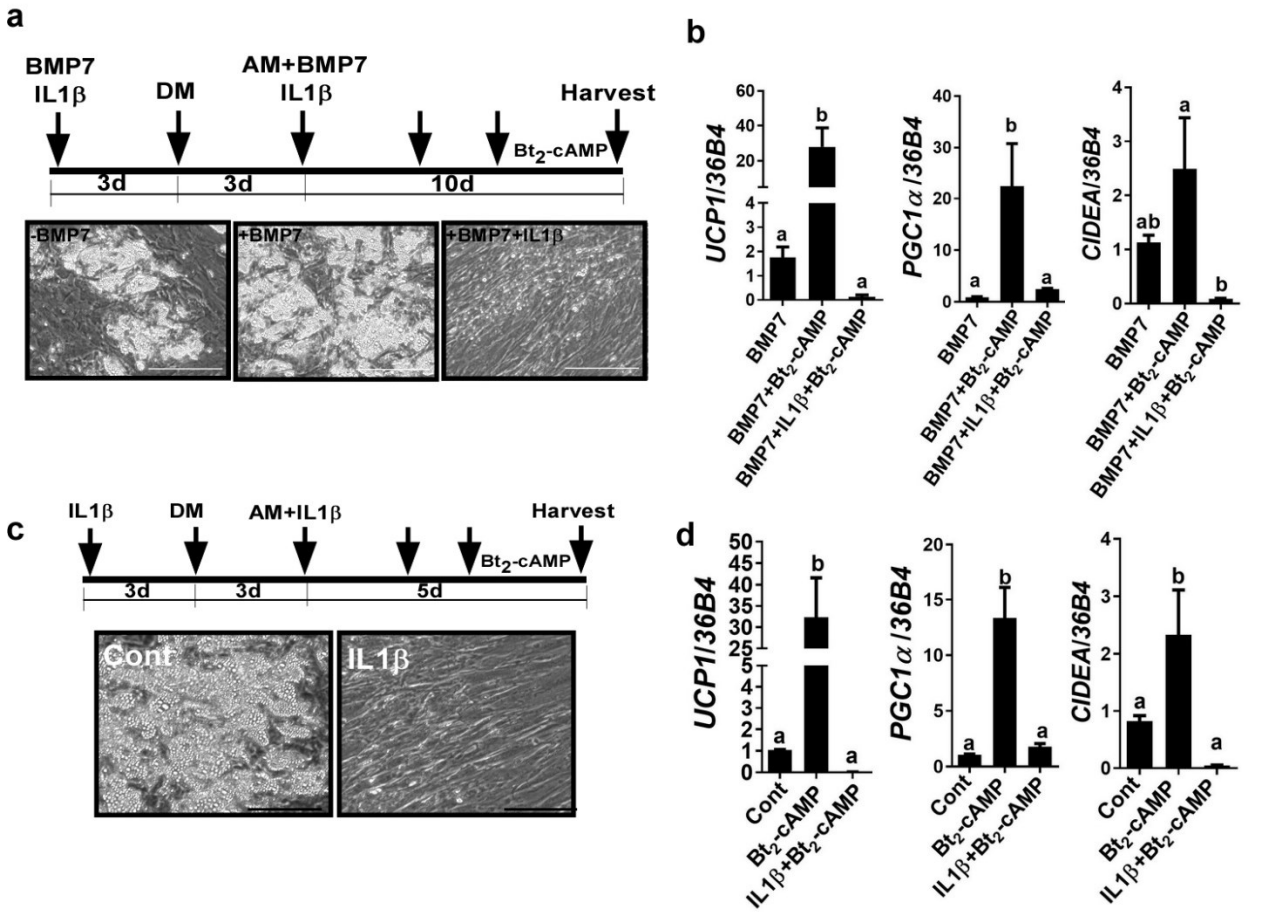

Supplementary Fig. 1. IL1β Interferes with BMP7- and Bt_2-cAMP-induced Human Beige Adipocyte Development. a-b. *h*ASC-derived adipocytes pre-exposed to BMP7 conditioned medium and human IL1β recombinant protein before and after differentiation until they became mature adipocytes and followed by Bt_2-cAMP stimulation. **a.** Phase contrast images for mature adipocytes (scale bar=400 μm). Arrows indicate the time line for BMP7 and IL1β addition and initiation of adipocyte differentiation by adding differentiation medium (DM) and adipocyte maintenance medium (AM). **b**. Relative gene expression analysis of *UCP1*, *PGC1α*, and *CIDEA* by qPCR. **c-d.** *h*ASC-derived adipocytes pre-exposed to human IL1β recombinant protein before differentiation and continuously after differentiation until they became mature adipocytes and followed by Bt_2-cAMP stimulation. **c.** Phase contrast images for mature adipocytes (scale bar=400 μm). Arrows indicate the time line for IL1β addition and initiation of adipocyte differentiation by adding differentiation medium (DM) and adipocyte maintenance medium (AM). **d**. Relative gene expression analysis of *UCP1*, *PGC1α*, and *CIDEA* by qPCR. All data are presented as mean ± SEM. Values not sharing a common letter differ significantly ($P<0.05$) by one-way ANOVA.